Pergamon

SCIENCE DIRECT®

Tetrahedron: *Asymmetry* 14 (2003) 1055–1061

TETRAHEDRON: *ASYMMETRY*

A tentative kinetic model for chiral amplification in autocatalytic alkylzinc additions

Thomas Buhse*

Centro de Investigaciones Químicas, Universidad Autónoma del Estado de Morelos, Av. Universidad No. 1001, Col. Chamilpa, 62210 Cuernavaca, Morelos, Mexico

Received 5 December 2002; accepted 27 January 2003

Abstract—A simplified kinetic model is proposed to describe stereoselective autocatalysis in specific alkylzinc additions. The model is based on current experimental knowledge and by the use of exclusively mono- or bimolecular processes attempting a chemically and kinetically realistic description. The underlying dynamics were expressed in terms of a template-directed self-replication in which a zinc alkoxide dimer acts as the active autocatalytic species. The model was shown to reproduce previously obtained kinetic data well, to address to the phenomenon of chiral amplification in a semi-quantitative manner, and to enlighten the cause of the effect of the initial enantiomeric excess on the globally observed kinetics. Amplification of enantiomeric excess occurs by considering a homogeneous and entirely symmetric reaction network.

1. Introduction

The observation of chiral autoamplification in specific alkylzinc additions — as pioneered by Soai and co-workers[1–6] has attracted close scientific interest for the description of highly nonlinear effects in asymmetric synthesis[7,8] as well as for possible model systems to explain the origin of biomolecular homochirality.[9,10] The prototype reaction (Scheme 1) consists of the addition of di-*iso*-propylzinc (Zn) to a pyrimidine-5-carbaldehyde (CHO) in the presence of a chiral and enantiomerically enriched 5-pyrimidyl alkanol (COH) as a catalyst to form the chiral *iso*-propylzinc alkoxide (COZn) usually with a significantly higher enantiomeric excess than that of the chiral auxiliary at the beginning of the reaction.

Since the catalyst and the product of the reaction (after hydrolysis) are structurally identical and furthermore an effect of enantioselective amplification has been observed, the above process can be considered as a striking example of asymmetric autocatalysis[11,12] in organic chemistry. Subsequent studies of Soai and co-workers showed that enantioselective amplification is not only restricted to the use of the chiral alcohol but can also be achieved by the addition of catalytic amounts of different organic[13] and inorganic[14,15] compounds. These results describe the way of directed

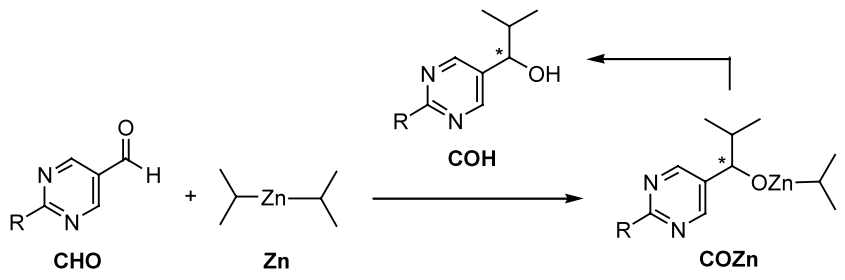

Scheme 1. Autocatalytic alkylzinc addition as proposed by Soai and co-workers.[1–6] R = H, Me, *t*-Bu-C≡C–.

* Corresponding author. Tel.: +52-777-3-29-79-97; fax: +52-777-3-29-79-97; e-mail: buhse@uaem.mx

0957-4166/03/$ - see front matter
doi:10.1016/S0957-4166(03)00128-9

chiral propagation that is of definite importance to unveil chiral implications, for example in prebiotic processes.

Despite the impact of the above findings, the mechanism of the prototype reaction has long been a subject of speculation. As an immediate assumption,[1] a Frank-type[16] amplification mechanism has been proposed that, however, would require not only the presence of an autocatalytic reaction network but also an extremely high degree of stereoselectivity[17] that is barely achieved in common asymmetric synthesis even in the presence of very active chiral catalysts. Furthermore, as recently demonstrated by Blackmond,[18] a Frank-type mechanism considering monomeric autocatalytic species such as COZn would always require the presence of mutual inhibition involving the two enantiomers, (*R*)-COZn+(*S*)-COZn, to achieve any effect of chiral amplification. However, the assumption of a reversible dimerization of the two monomers forming homo- and heterochiral dimers and allowing them to play the role of active catalytic species renders the dynamics of the reaction network much more subtle and would additionally shed a different light on the simple form of mutual inhibition as stated in the Frank model. In fact, recent kinetic studies[19,20] indicate the involvement of a catalytically active dimeric species composed of two *iso*-propylzinc alkoxide molecules, $(COZn)_2$, that probably acts as the actual chiral catalyst. These new results allow a more detailed kinetic analysis.

The aim of this paper is to propose a simplified kinetic model for the prototype reaction (Scheme 1) that is based on previously observed experimental kinetic data and that describes the reaction mechanism as a variation of a template-directed autocatalytic system that is usually proposed for artificial self-replicating systems.[21–23] This basic assumption could explain the origin of the high stereoselectivity that is needed for effective chiral amplification. Self-replicating systems commonly exhibit very high specificity due to the presence of a truly 'selfish' autocatalyst. Furthermore, as has been recently shown for a chiroselective peptide self-replicator,[24] these systems can display effective chiral information transfer bypassing the production of noise such as observed in more classical autocatalytic reactions.

2. Kinetic modeling

2.1. Kinetic core model

To reproduce the experimentally observed kinetic data,[19] a kinetic core model (Table 1) has been designed. The model takes into account the formation of the product species (COZn) via two formally distinct pathways: a direct and uncatalyzed background route (steps I and II) as well as an autocatalytic pathway (steps III–V).

The direct route consists of alkylzinc (Zn) addition to the initially added alcohol (COH) that can be considered to proceed very rapidly, and the noncatalyzed addition of Zn to the aldehyde (CHO), which is probably a very slow or even negligible process that is readily overshadowed by the autocatalytic processing.

The autocatalytic network reflects two association processes that have been discussed previously[19,20] namely, the dimerization of COZn and the association of CHO to the dimer species. These two processes have been considered to be reversible without a priori specifying that the rate of equilibration was fast or slow. In this context, $(COZn)_2$ acts as a template species that can associate the two reactants: CHO in step IV and Zn in step V. Step V describes in a condensed way this second association and the immediate release of COZn and of free $(COZn)_2$ that can act again as a template in the subsequent autocatalytic cycle. In essence, the template dimer acts as a catalyst assisting the coupling between CHO and Zn that have been associated to $(COZn)_2$. As outlined in Scheme 2, the autocatalytic cycle represents an effective machinery for an increasing formation of COZn during the course of the reaction.

Table 1. List of processes, reactions and corresponding rate laws in the kinetic core model

Process	Reaction	Rate law	Step
Irreversible formation of the zinc alkoxide	$COH + Zn \rightarrow COZn$ $CHO + Zn \rightarrow COZn$	$R_I = k_1$ [COH] [Zn] $R_{II} = k_2$ [CHO] [Zn]	I II
Reversible zinc alkoxide dimerization equilibrium	$COZn + COZn \leftrightarrow (COZn)_2$	$R_{IIIa} = k_3$ $[COZn]^2$ $R_{IIIb} = k_{-3}$ $[(COZn)_2]$	III a III b
Reversible association of the carbaldehyde	$(COZn)_2 + CHO \leftrightarrow (COZn)_2$–CHO	$R_{IVa} = k_4$ $[(COZn)_2]$ [CHO] $R_{IVb} = k_{-4}$ $[(COZn)_2$-CHO]	IV a IV b
Irreversible catalyzed formation of the zinc alkoxide	$(COZn)_2$–CHO + Zn $\rightarrow (COZn)_2 + COZn$	$R_V = k_5$ $[(COZn)_2$–CHO] [Zn]	V
Side reaction	$COH + CHO \rightarrow P$	$R_{VI} = k_6$ [COH][CHO]	VI

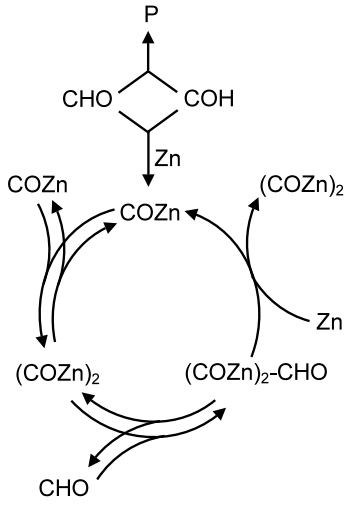

Scheme 2. Representation of the proposed kinetic core model describing the reaction system in terms of a template-directed autocatalytic process.

Although chemically uncertain, step VI stands dynamically for the experimental observation[19] that the concentration of COZn after the reaction is complete was always less than that of the limiting reactant CHO. Based on the restricted number of species considered for the kinetic model and on the circumstance that the discrepancy between the expected and observed final product concentrations apparently increases on increasing the concentration of the initial alcohol, a formal side reaction between CHO and COH has been included. This step was shown in test simulations to be the only suitable one for the consistent reproduction of kinetic data coming from different experimental settings. As indicated by Soai and co-workers, who used a control parameter with different values for each experimental setting in their empirical model[19] to circumvent this discrepancy, the chemical origin of this effect still seems to be unknown and requires further investigation.

2.2. Chiral processing

The kinetic model, which includes the chiral processing to describe the observed enantiomeric amplification (Table 2), has been directly derived from the core model.

The addition of Zn to (*R*)- or (*S*)-COH (step C-I) was assumed to occur with complete conservation of the absolute configuration with respect to the product (*R*)- or (*S*)-COZn. Kinetically, this step is entirely symmetric so that under racemic initial conditions, i.e. $[(R)\text{-COH}]_0 = [(S)\text{-COH}]_0$, the outcome would also be racemic, while step C-II always generates *rac*-COZn.

For the dimerization of COZn (step C-III), the occurrence of a different degree of stereoselectivity between the homochiral association, (*R*)+(*R*) or (*S*)+(*S*), and the heterochiral dimerization, (*R*)+(*S*), was allowed by introducing the dimensionless stereoselective parameter α. Due to the lack of definite experimental data, this reasoning was based on structural arguments that may cause differences in the rate between the formation of the enantiomerically pure and diastereomeric dimeric species. If $\alpha < 1$, the homochiral dimerization would be favored over the heterochiral one and if $\alpha > 1$ the opposite would be true. For the case $\alpha = 1$, step C-III would proceed without any homochiral or heterochiral preference, as is the case for the corresponding dissociation reactions, for which the same rate constant, k_{-3}, has always been considered. It should also be noted that (*R*)(*S*)-$(COZn)_2$ and (*S*)(*R*)-$(COZn)_2$ are chemically equivalent so that only one species appears in the kinetic scheme.

Completely symmetrical kinetic behavior was further considered for the association of CHO to the hetero- and homochiral $(COZn)_2$ and for the respective dissociation as expressed by the unique rate constants k_4 and k_{-4} (step C-IV).

Step C-V describes the catalyzed formation of (*R*)- and (*S*)-COZn in terms of complete stereospecifity if originating from the homochiral dimer species, i.e., the association of Zn to the (*R*)(*R*) dimer generates exclusively (*R*)-COZn+(*R*)(*R*)-$(COZn)_2$ and the (*S*)(*S*) dimer solely (*S*)-COZn+(*S*)(*S*)-$(COZn)_2$, respectively. This assumption can be considered as chemically overstated

Table 2. Reaction steps and corresponding rate parameters used for the kinetic model including chiral processing

Reaction	Rate parameter	Step
(*R*)-COH + Zn → (*R*)-COZn	(k_1)	C-I
(*S*)-COH + Zn → (*S*)-COZn	(k_1)	
CHO + Zn → (*R*)-COZn	(k_2)	C-II
CHO + Zn → (*S*)-COZn	(k_2)	
(*R*)-COZn + (*R*)-COZn ↔ (*R*)(*R*)-$(COZn)_2$	(k_3, k_{-3})	C-III
(*S*)-COZn + (*S*)-COZn ↔ (*S*)(*S*)-$(COZn)_2$	(k_3, k_{-3})	
(*R*)-COZn + (*S*)-COZn ↔ (*R*)(*S*)-$(COZn)_2$	($\alpha \times k_3$, k_{-3})	
(*R*)(*R*)-$(COZn)_2$ + CHO ↔ (*R*)(*R*)-$(COZn)_2$–CHO	(k_4, k_{-4})	C-IV
(*S*)(*S*)-$(COZn)_2$ + CHO ↔ (*S*)(*S*)-$(COZn)_2$–CHO	(k_4, k_{-4})	
(*R*)(*S*)-$(COZn)_2$ + CHO ↔ (*R*)(*S*)-$(COZn)_2$–CHO	(k_4, k_{-4})	
(*R*)(*R*)-$(COZn)_2$–CHO + Zn → (*R*)(*R*)-$(COZn)_2$ + (*R*)-COZn	(k_5)	C-V
(*S*)(*S*)-$(COZn)_2$–CHO + Zn → (*S*)(*S*)-$(COZn)_2$ + (*S*)-COZn	(k_5)	
(*R*)(*S*)-$(COZn)_2$–CHO + Zn → (*R*)(*S*)-$(COZn)_2$ + (*S*)-COZn	(k_5)	
(*R*)(*S*)-$(COZn)_2$–CHO + Zn → (*R*)(*S*)-$(COZn)_2$ + (*R*)-COZn	(k_5)	
(*R*)-COH + CHO → P	(k_6)	C-VI
(*S*)-COH + CHO → P	(k_6)	

but has been made for the sake of simplicity in order to restrict the model system to one single stereoselective parameter (α). In contrast to this, the interaction between the heterochiral (R)(S) dimer and Zn results in a racemic outcome.

The side reaction C-VI was assumed to occur without any preference for (R)- or (S)-COH.

2.3. Computations

Model calculations, as described in the following sections, were performed with Sa (version 2.0)[25] on a personal computer. The general algorithm used for the numerical integration of the differential equations was based on a semi-implicit Runge–Kutta method and the basic optimization procedure using a nonlinear minimization algorithm for the adjustment of the rate parameters of the model to the experimental data has been described elsewhere.[17,26,27]

2.4. Reproduction of experimental data

Using the core model (Table 1), it was attempted to reproduce simultaneously, i.e. with the same set of rate parameters, the experimentally observed data[19] of two experimental settings in which different initial concentrations of COH have been used. Both experiments have been reportedly performed under identical experimental conditions at $T=0$°C while a third one was carried out at $T=-45$°C. As shown in Fig. 1, the kinetic model performed an acceptable reproduction of the observed kinetic curves. A similar conformity has also been achieved for the experiment at $T=-45$°C (not shown), obviously resulting in a different set of rate parameters. For the kinetic modeling, it was assumed that the published experimental values of the product concentrations reflect a complete dissociation of all dimeric COZn species at the time when the reaction was experimentally quenched. Thus, for the modeling it was considered that the product concentrations as plotted were the sum of all COZn, $[\mathrm{COZn}]_{tot}=[\mathrm{COZn}]+2\times[(\mathrm{COZn})_2]+2\times[(\mathrm{COZn})_2\text{–CHO}]$.

It turned out that the offset in the induction period and the steep rate increase observed for experiments (1) and (2), see Fig. 1, was impossible to reproduce by a simplified autocatalytic model scheme considering monomeric COZn instead of dimeric $(\mathrm{COZn})_2$ as the catalytic species. This observation is in agreement with a previous attempt by Soai and co-workers[19] as well as by Blackmond et al.[20] and validates the assumption of a self-replication-like mechanism.

The above experiments did not allow the product enantiomers (R)-COZn and (S)-COZn to be distinguished and furthermore all experiments were performed under almost enantiomerically pure initial conditions, i.e. (S)-COH>99.5% ee. To account for chiral amplification effects by the extended model (Table 2) a semi-quantitative prediction of the results of prototype experiment 'B3'[1] was attempted. These simulations (Fig. 2) were performed by using the fixed values for the rate con-

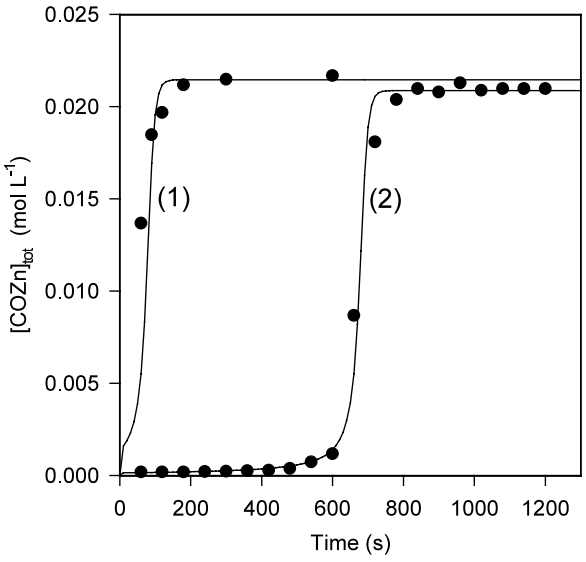

Figure 1. Kinetics of product formation in autocatalytic alkylzinc addition. Filled circles: experimental data.[19] Solid lines: reproduction of experimental data by the kinetic core model as shown in Table 1. Initial conditions ($T=0$°C): $[\mathrm{CHO}]=2.08\times10^{-2}$ M, $[\mathrm{Zn}]=3.13\times10^{-2}$ M, $[\mathrm{COH}]=2.08\times10^{-3}$ M (curve 1), $[\mathrm{COH}]=2.08\times10^{-4}$ M (curve 2). Adjusted rate parameters (rounded): $k_1=1.0\times10^4$ M^{-1} s^{-1}, $k_2=1.0\times10^{-5}$ M^{-1} s^{-1}, $k_3=8.0\times10^2$ M^{-1} s^{-1}, $k_{-3}=1.1\times10^2$ s^{-1}, $k_4=1.0\times10^2$ M^{-1} s^{-1}, $k_{-4}=1.0\times10^2$ s^{-1}, $k_5=8.0\times10^3$ M^{-1} s^{-1}, $k_6=7.8\times10^3$ M^{-1} s^{-1}.

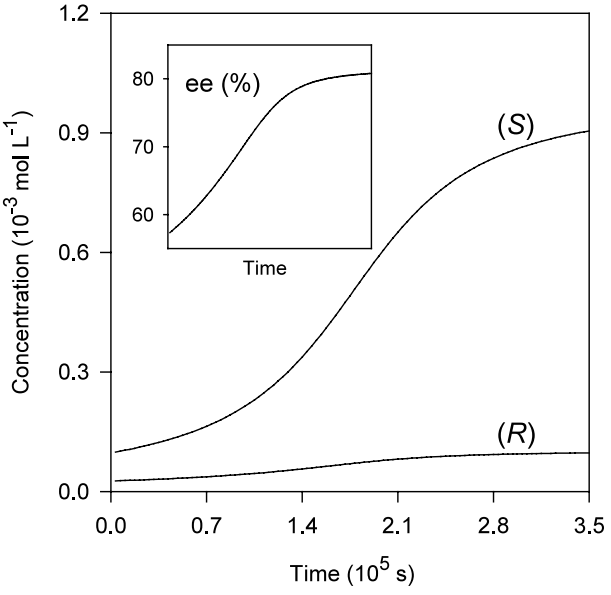

Figure 2. Simulated time evolution of [(S)-COZn] and [(R)-COZn] by the kinetic model presented in Table 2. Insert: corresponding time evolution of the enantiomeric excess (same time scale). Initial conditions taken from Ref. 1: $[\mathrm{CHO}]=1.04\times10^{-3}$ M, $[\mathrm{Zn}]=1.20\times10^{-3}$ M, $[(S)\text{-COH}]=1.634\times10^{-4}$ M, $[(R)\text{-COH}]=4.462\times10^{-5}$ M; $ee_0=57.1\%$. Same set of rate parameters as given in Fig. 1, $\alpha=0.45$.

stants obtained by the data reproduction as shown in Fig. 1 but allowing variations in the parameter α. Prior to these simulations, it was confirmed that values of $\alpha \neq 1$ did not substantially affect the former data adjustment (i.e. in the core model $\alpha = 1$).

As shown in Fig. 2, the enantiomeric excess in respect to (*S*)-COZn climbs from initially $ee_0 = 57\%$ to $ee = 81\%$ as reported for the experimental outcome.[1] For this case the stereoselective parameter was set to $\alpha = 0.45$. The simulated concentrations of $[(S)\text{-COZn}] = 9.2\times10^{-4}$ M and $[(R)\text{-COZn}] = 9.8\times10^{-5}$ M after 96 h of reaction time turned out to be very close to the actually observed concentrations ($[(S)\text{-COZn}]_{obs} = 7.6\times10^{-4}$ M and $[(R)\text{-COZn}]_{obs} = 7.1\times10^{-5}$ M). This indicates the capacity of the model also to reproduce observed chiral amplification effects in a semi-quantitative manner.

3. Dynamic properties

3.1. Reaction fluxes and autocatalytic effect

The reaction fluxes R_I to R_{VI} and the corresponding concentrations of the involved species have been analyzed at about the rate maximum corresponding to the kinetic curves shown in Fig. 1. The fluxes R_I and R_{VI} were found to be virtually at zero because of the rapid and total depletion of COH during the very initial stage of the reaction. For the remaining fluxes, the following order emerged: $R_{IIIa} \cong R_{IIIb} > R_{IVa} > R_V > R_{IVb} \gg R_{II}$ and for the concentrations of the species: Zn (as an excess reactant)>COZn>CHO>$(COZn)_2 \gg (COZn)_2$–CHO.

The main fluxes of the reaction network are obviously located in the autocatalytic cycle while the background reaction to produce COZn (step II) plays a negligible role. The strongest and bidirectional fluxes appear for the COZn+COZn↔$(COZn)_2$ dimerization equilibrium (step III, $K_{eq} = 7.63$) that basically acts to adjust the concentration of the catalytic dimer $(COZn)_2$ against the concentration of the noncatalytic COZn monomer. As typical for self-replicating systems, dimerization of the product species usually leads to a decrease in the autocatalytic effect (product inhibition)—in the present case, however, it is the dissociation of the dimer that decreases the autocatalytic strength. Essentially, step III can be regarded as a trigger for the autocatalytic efficiency of the system, i.e. the more it is shifted to the dimer species the stronger the autocatalytic effect is.

It turns out that at rate maximum the concentration of $(COZn)_2$ is about one order of magnitude less than that of COZn. This difference is small compared to typical self-replicating systems in which the concentration of the catalytic species is generally several orders of magnitude less than that of the noncatalytic dimer.[26,27] This explains the comparatively pronounced autocatalytic efficiency observed for the reaction system under consideration in contrast to the usually weak autocatalytic dynamics of prototype self-replicating systems. The relatively strong autocatalytic effect also becomes easily visible by regarding the distinct sigmoidal shape of the kinetic curves shown in Fig. 1 that is generally missing in typical self-replicating systems.

3.2. Chiral amplification and the kinetic effect of the initial enantiomeric excess

Following the simulation results, the dynamics of chiral amplification are basically governed by both a comparatively strong autocatalytic effect and a marked stereoselectivity.

The model simulations indicate that the kinetics of the total product formation, (*R*)-COZn+(*S*)-COZn, are a function of the enantiomeric excess of the initially added COH. This has been already observed by Blackmond et al.[20] by experiment. The effect has been monitored even for the case in which the initial concentration of the alcohol in total, $[(R)\text{-COH}+(S)\text{-COH}]_0$, was kept constant and only the ratio between the two enantiomers has been varied. As shown in Fig. 3, the reaction appears to proceed increasingly faster if the initial enantiomeric excess of the alcohol was increased.

By roughly inspecting the lag period of the two kinetic curves shown in Fig. 3, the average rates during the first 500 s of reaction time show a marked difference: the rate of the enantiomerically pure scenario is approximately twice that of the reaction started under racemic initial conditions. However, the rate maximum for both cases appears to be virtually the same. This effect is reminiscent of a typical autocatalytic system in which different amounts of an autocatalyst were initially added.

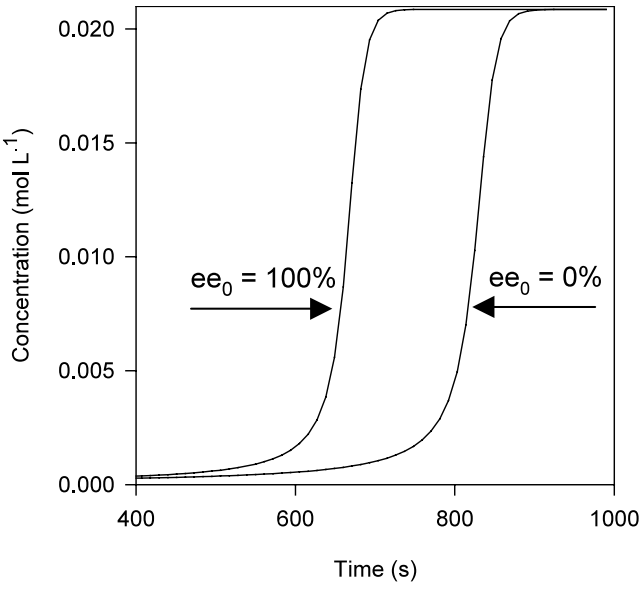

Figure 3. Effect of the initial enantiomeric excess on the kinetics of total product formation $[(COZn)_{tot}]$. Initial conditions: $[CHO] = 2.08\times10^{-2}$ M, $[Zn] = 3.13\times10^{-2}$ M; left curve: $[(S)\text{-COH}] = 2.08\times10^{-4}$ M, $[(R)\text{-COH}] = 0$ M; right curve: $[(S)\text{-COH}] = 1.04\times10^{-4}$ M, $[(R)\text{-COH}] = 1.04\times10^{-4}$ M. Same set of rate parameters as given in Fig. 1, $\alpha = 1$.

This effect is essentially due to the involved chiral implications and can be traced back to the bimolecular processes in step C-III (Table 2). A simple evaluation shows that in this step the total yield of $(COZn)_2$ is at maximum for enantiomerically pure initial conditions and at minimum for racemic ones, where the ratio in the theoretical yield before entering the autocatalytic cycle is 1:0.75; for the sake of simplicity, not considering the non-discriminative direct formation of COZn in step C-II. Note that there is no immediate difference in the catalytic 'power' between the homochiral and the heterochiral dimer species but a rapidly established difference in the concentration in respect to the total amount of the catalytic species. Subsequently, this difference undergoes amplification during the course of the autocatalytic cycle and becomes increasingly larger. In other words it is not necessary to assume that the homochiral and heterochiral catalyst dimer are embedded in two distinct reaction pathways (e.g. a catalytic and a noncatalytic one). In fact, it is the same reaction network for both but the presence of the bimolecular processes in step C-III that initiates the difference in the kinetics *before* the actual autocatalytic process starts.

3.3. Factors affecting chiral amplification and the product enantiomeric excess

Concerning the model system (Table 2), basically three factors account for chiral amplification and for the observed degree in enantiomeric excess: 1. the above mentioned step C-III favoring the excess enantiomer over the minor one followed by its amplification in the autocatalytic cycle; 2. the value of the stereoselective parameter α.; and 3. the stereospecifity considered for step C-V.

A closer examination of the dynamics of step C-III leads to the assumption that in respect to the heterochiral dimerization, (*R*)-COZn+(*S*)-COZn↔(*R*)(*S*)-$(COZn)_2$, two opposing factors could affect the enantiomeric excess of the catalytic species that are subsequently available for the autocatalytic cycle. In the presence of this process ($\alpha>0$), equimolar amounts of both (*R*)- and (*S*)-COZn enantiomers form the heterochiral dimer. Consequently, this leads to an increase in the enantiomeric excess of the major enantiomeric monomer species in a way that is analogous to a racemate crystallization.[28–30] On the other hand, in the absence of the respective process ($\alpha=0$), exclusively the formation of the homochiral dimer is possible that also leads to an amplification of the enantiomeric excess due to the stereospecifity in step C-V. Obviously, the first process is soon overshadowed by the second one as shown in Fig. 4 in which the product enantiomeric excess (ee_{prod}) does not decrease but increases by diminishing the value of α.

It is interesting to note that a positive nonlinear effect of ee_{prod} versus ee_0 is obtained even for the case in which $\alpha=1$ (see Fig. 4). This means that it is theoretically possible to describe autocatalytic chiral amplification by the model scheme by keeping entire symmetry corresponding to all involved rate parameters. However, amplification effects as quantitatively observed by Soai and co-workers[1–6] apparently require a value of $\alpha<1$ as already shown in Fig. 2. In respect to the model system, this indicates that the dimerization (step C-III) probably proceeds in a stereoselective way, favoring the formation of the homochiral over the heterochiral dimer. This is in agreement with the findings of Blackmond and co-workers[18,20] who demonstrated experimentally that there is no disposition toward a more stable heterochiral dimer.

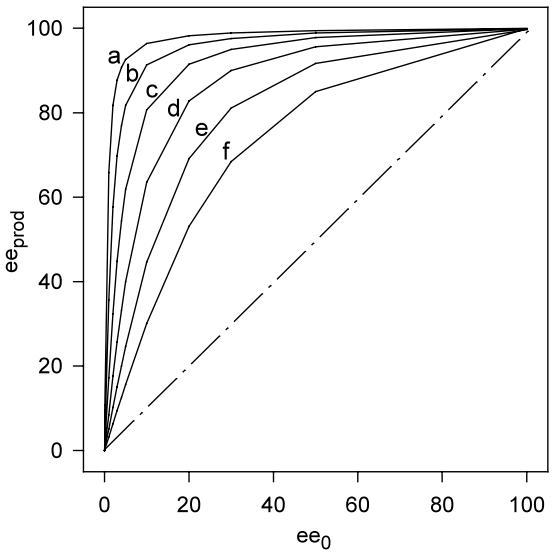

Figure 4. Nonlinear relationship between product enantiomeric excess (ee_{prod}) and enantiomeric excess of initially added ROH (ee_0) as a function of the stereoselective parameter. Curves a→f: $\alpha=0$, 0.2, 0.4, 0.6, 0.8, 1.0. The broken line indicates the optimum case for a linear relationship.

4. Conclusion

A simplified kinetic model to account for chiral amplification in autocatalytic alkylzinc additions has been proposed. The model describes for the first time the possible reaction network by the use of exclusively mono- and bimolecular processes and by taking reversible processes into account without a priori assuming that equilibration occurred fast or slow. Most of these processes can be traced back to rational chemical reactions.

The basic dynamics of the reaction system were expressed in terms of a self-replication-type mechanism in which the zinc alkoxide dimer, $(COZn)_2$, plays the central role as a template species that can associate CHO and Zn and consequently catalyzes the formation of COZn. Applying the method of inverse data treatment, the above consideration has led to an acceptable reproduction of experimentally studied kinetics and could describe the kinetic effect of the initially added enantiomeric excess on the globally observed kinetics. This allowed closer analysis of the possible dynamic properties of the reaction system.

It was shown that the comparatively high concentration of the catalytic dimer causes the pronounced autocatalytic efficiency that is untypical for usual self-replicating systems but that is apparently essential for chiral amplification phenomena. It turns out that even an entirely symmetric reaction network can cause enantiomeric amplification and that it is unnecessary to assume different pathways for homochiral vs. heterochiral processing. In essence, autocatalysis and chiral amplification cannot be reduced to a single step but the whole kinetic scheme has to be taken into account. This also concerns the proposed[18] fundamental requirement of a mechanism for suppression of production of the minor enantiomer that in a simple Frank-type model is obvious but in the present case apparently embedded in the dynamic dimerization equilibria.

Although representing a more detailed dynamic description of chiral amplification in alkylzinc additions, the proposed model remains tentative because of a number of still uncharacterized chemical processes and the lack of more extensive kinetic data. It is proposed that future experiments should focus on different aspects like the role of side reactions, the dimerization processes as well as the thermodynamic properties of the assumed dimers and above all: the time evolution of single enantiomeric species.

Acknowledgements

The author acknowledges gratefully financial support by the Consejo Nacional de Ciencia y Tecnología of México (CONACyT)-research grant 34236-E.

References

1. Soai, K.; Shibata, T.; Morioka, H.; Choji, K. *Nature* **1995**, *378*, 767–768.
2. Shibata, T.; Choji, K.; Hayase, T.; Aizu, Y.; Soai, K. *Chem. Commun.* **1996**, 1235–1236.
3. Shibata, T.; Morioka, H.; Hayase, T.; Choji, K.; Soai, K. *J. Am. Chem. Soc.* **1996**, *118*, 471–472.
4. Shibata, T; Hayase, T.; Yamamoto, J.; Soai, K. *Tetrahedron: Asymmetry* **1997**, *8*, 1717–1719.
5. Soai, K.; Shibata, T. In *Advances in BioChirality*; Pályi, G.; Zucchi, C.; Caglioti; L., Eds. Asymmetric autocatalysis and biomolecular chirality. Elsevier: Amsterdam, 1999; pp. 125–136.
6. Soai, K.; Shibata, T.; Sato, I. *Acc. Chem. Res.* **2000**, *33*, 382–390.
7. Avalos, M.; Babiano, R.; Cintas, P.; Jiménez, J. L.; Palacios, J. C. *Tetrahedron: Asymmetry* **1997**, *8*, 2997–3017.
8. Girard, C.; Kagan, H. B. *Angew. Chem., Int. Ed.* **1998**, *37*, 2922–2959.
9. Bonner, W. A. *Origins Life Evol. Biosphere* **1991**, *21*, 59–111.
10. Keszthely, L. *Quart. Rev. Biophys.* **1995**, *28*, 473–507.
11. Avalos, M.; Babiano, R.; Cintas, P.; Jiménez, J. L.; Palacios, J. C. *Tetrahedron: Asymmetry* **2000**, *11*, 2845–2874.
12. Kondepudi, D. K.; Asakura, K. *Acc. Chem. Res.* **2001**, *34*, 946–954.
13. Shibata, T.; Yamamoto, J.; Matsumoto, N.; Yonekubo, S.; Osanai, S.; Soai, K. *J. Am. Chem. Soc.* **1998**, *120*, 12157–12158.
14. Soai, K.; Osanai, S.; Kadowaki, K.; Yonekubo, S.; Shibata, T.; Sato, I. *J. Am. Chem. Soc.* **1999**, *121*, 11235–11236.
15. Sato, I.; Kadowaki, K.; Soai, K. *Angew. Chem., Int. Ed.* **2000**, *39*, 1510–1512.
16. Frank, F. C. *Biochim. Biophys. Acta* **1953**, *11*, 459–463.
17. Buhse, T.; Lavabre, D.; Micheau, J. C.; Thiemann, W. *Chirality* **1993**, *5*, 341–345.
18. Blackmond, D. G. *Adv. Synth. Catal.* **2002**, *344*, 156–158.
19. Sato, I.; Omiya, D.; Tsukiyama, K.; Ogi, Y.; Soai, K. *Tetrahedron: Asymmetry* **2001**, *12*, 1965–1969.
20. Blackmond, D. G.; McMillan, C. R.; Ramdeehul, S.; Schorm, A.; Brown, J. M. *J. Am. Chem. Soc.* **2001**, *123*, 10103–10104.
21. Orgel, L. E. *Nature* **1992**, *358*, 203–209.
22. Bag, B. G.; von Kiedrowski, G. *Pure Appl. Chem.* **1996**, *68*, 2145–2152.
23. Robertson, A.; Sinclair, A. J.; Philip, D. *Chem. Soc. Rev.* **2000**, *29*, 141–152.
24. Saghatelian, A.; Yokobayashi, Y.; Soltani, K.; Ghadiri, M. R. *Nature* **2001**, *409*, 797–801.
25. Sa (Simulation+adjustment) is a non-commercial program based on C^{++} that was developed at the Laboratoire de IMRCP, Université Paul Sabatier, Toulouse, France.
26. Rivera Islas, J; Pimienta, V.; Micheau, J. C.; Buhse, T. *Biophys. Chem.* **2003**, in press.
27. Rivera Islas, J; Pimienta, V.; Micheau, J. C.; Buhse, T. *Biophys. Chem.* **2003**, in press.
28. Jacques, J.; Collet, A.; Wilen, S. H. *Enantiomers, Racemates and Resolution*; Wiley: New York, 1981.
29. Bernal, I. *J. Chem Educ.* **1992**, *69*, 468–469.
30. Buhse, T.; Kondepudi, D. K.; Hoskins, B. *Chirality* **1999**, *11*, 343–348.